Hindawi
Shock and Vibration
Volume 2023, Article ID 9950270, 12 pages
https://doi.org/10.1155/2023/9950270

Research Article

Fractional Order Derivative and Time-Delay Feedback Enabled Stochastic Resonance for Bearing Fault Diagnosis

Yidan Mei,[1] **Lutie Chen**,[1] **Wentao Xu**,[1] **Chao Liu**,[2] **Zijian Qiao**,[1,3,4] **and Zhihui Lai**[5]

[1]*CATARC Automotive Component Test Center (Ningbo) Co., Ltd., Ningbo 315104, China*
[2]*College of Mechanical and Electrical Engineering, Gansu Forestry Polytechnic, Tianshui 741020, China*
[3]*Yangjiang Offshore Wind Power Laboratory, Yangjiang 529500, Guangdong, China*
[4]*Zhejiang Provincial Key Laboratory of Part Rolling Technology, School of Mechanical Engineering and Mechanics, Ningbo University, Ningbo 315211, Zhejiang, China*
[5]*Shenzhen Key Laboratory of High Performance Nontraditional Manufacturing, College of Mechatronics and Control Engineering, Shenzhen University, Shenzhen 518060, China*

Correspondence should be addressed to Chao Liu; chaoliugl@hotmail.com and Zijian Qiao; qiaozijian@nbu.edu.cn

Received 6 July 2023; Revised 17 August 2023; Accepted 26 September 2023; Published 10 October 2023

Academic Editor: Cecilia Surace

The benefits of noise can be found in nonlinear systems where a type of resonances can inject the noise into systems to enhance weak signals of interest, including stochastic resonance, vibrational resonance, and chaotic resonance. Such benefits of noise can be improved further by adding some items into the nonlinear systems. Considering the time-dependent memory of fractional-order derivative and time-delay feedback which makes the nonlinear systems take advantage of their historical information and makes the output of nonlinear systems affect the input by feedback control, therefore, we attempt to design the model of stochastic resonance (SR) enhanced by both fractional-order derivative and time-delay feedback. Among them, fractional-order derivative and time delay would reinforce the memory of nonlinear systems for historical information and feedback would use the output of systems to control the systems precisely. Therefore, we hope that their advantages would be fused to improve the weak signal detection performance of SR further. Then, it would be applied to bearing fault diagnosis and compared with that without fractional-order derivative and time-delay feedback and even other diagnostic methods. The experimental results indicate that the SR enhanced by fractional-order derivative and time-delay feedback where a local signal-to-noise ratio is designed as the objective function to optimize these tuning parameters of the proposed method could enhance early fault signature of bearings and outperform that without fractional-order derivative and time-delay feedback and even infogram method.

1. Introduction

Stochastic resonance (SR) is a kind of nonlinear phenomena where noise is injected into nonlinear systems to enhance their outputs [1]. Therefore, SR lets us discover the benefits of noise [2]. With the development of research, it is found that there are lots of the benefits of noise in real world in addition to SR [3], for example chaotic resonance [4–6] and vibrational resonance [7]. Such a behavior has attracted sustaining attention to apply it into various fields such as image enhancement [8], information transmission [9], and fault detection and fault diagnosis of rotating machinery [10–13], especially the development and future directions of SR in machine fault diagnosis have been summarized and proposed by [10, 14].

Among them, SR-based fault detection and fault diagnosis has become one of the most widely studied and applied directions. They can be categorized into novel potentials [15], novel nonlinear systems [16], novel behaviors [17], novel methodologies [18], and others. Because this paper focuses on improving novel nonlinear systems, we would review the development of novel nonlinear systems, which mainly contains two aspects.

On the one hand, some scholars attempt to add the fractional-order derivative into nonlinear systems to induce

more abundant dynamics for better weak signal detection than those without fractional-order derivative. For example, Zheng et al. applied genetic algorithms to optimize the multi parameters of fractional-order SR for weak signal detection [19]. Yang et al. investigated stochastic P-bifurcation and SR in fractional-order bistable nonlinear systems, indicating that the fractional-order SR can enhance the weak signal better than integral-order ones [20]. Zeng et al. designed a new indicator, namely, weighted correctional signal-to-noise ratio, to tune the parameters of fractional-order SR for mechanical fault diagnosis [21]. Qiao et al. employed the fractional-order derivative to improve the second-order SR for enhancing weak fault signature of machinery [22]. Guo et al. studied the effect of random mass and signal-modulated noise on SR in fractional-order harmonic oscillators [23]. Yu et al. explored the SR in two coupled fractional harmonic oscillators induced by a dichotomous fluctuating mass, indicating that coupling strength and the fractional order both benefit to weak signal detection [24]. Zhong et al. studied the collective SR in globally coupled fractional-order harmonic oscillators induced by multiplicative noise [25]. The above researches indicated that the fractional-order derivative is able to improve SR for weak signal detection than integral-order ones.

On the other hand, time delay can utilize the historical information of nonlinear systems to enhance weak signal detection, whereas feedback could achieve the precise control of nonlinear systems for improving the output. Therefore, some scholars pay more attention to studying the SR with time delay and feedback. For example, Wu and Zhu investigated the SR in a bistable system with time-delayed feedback driven by non-Gaussian noise by using two indicators including quasi-steady-state probability distribution function and signal-to-noise ratio (SNR) [26]. Lu et al. proposed a time-delayed feedback SR method for mechanical fault diagnosis [27]. Shi et al. presented a time-delayed tristable SR method for mechanical fault diagnosis, suggesting that time delay and feedback affect the noise enhanced stability [28]. Meanwhile, Shi et al. designed a high-order time-delayed feedback tristable SR method for enhancing weak fault signature [29]. Wadop Ngouongo et al. reported the SR with memory effects in a deformation potential [30]. Wang et al. studied the effect of fractional damping and time-delayed feedback on SR [31]. Li et al. studied the time-delayed feedback monostable SR in bearing fault diagnosis by fusing minimum entropy deconvolution [32]. Wang et al. explored the influences of time-delayed feedback on logical SR and the results indicated that the delay time can enhance the output SNR [33]. Yang et al. indicated that the time delay can control primary resonance and SR, and increasing feedback intensity can suppress the vibrations [34]. Liu et al. proposed a controlled SR method with time-delayed feedback to enhance weak fault signature of machinery [35]. In sum, both time delay and feedback can improve the weak signal detection of SR by precise control and information memory.

The above summary of literature has indicated that both fractional-order derivative and time-delayed feedback can improve the weak signal detection of SR from historical information memory, precise control, and so on. Up to now, however, the SR with both fractional-order derivative and time-delayed feedback has not been studied and applied to mechanical fault diagnosis yet. Therefore, this paper attempts to fuse their advantages to improve the weak signal detection of SR further, thereby enhancing the weak early fault signature of the machinery. Inspired by such an idea, the remainder of this paper is organized as follows. Section 2 designs a SR model enhanced by fractional-order derivative and time-delay feedback and provides its mathematical expression. In Section 3, we apply the SR enhanced by fractional-order derivative and time-delay feedback to bearing fault diagnosis and a bearing fault experiment is performed to demonstrate its effectiveness and feasibility. Even the comparison between those with or without fractional-order derivative and time-delay feedback is made. Finally, conclusions are drawn in Section 4.

2. An SR Model Enhanced by Fractional-Order Derivative and Time-Delay Feedback

The existing nonlinear systems of SR are of two kinds: overdamped and underdamped ones [36]. Overdamped SR characterizes the low-pass filtering properties [37, 38], while underdamped SR characterizes the band-pass filtering properties which is more suitable to enhance weak signals under strong background noise than overdamped ones [39, 40]. Hence, we pay attention to underdamped SR and it can be described as follows:

$$\frac{\mathrm{d}^2x}{\mathrm{d}t^2} + \gamma\frac{\mathrm{d}x}{\mathrm{d}t} = -\frac{\partial U(x)}{\partial x} + A\cos\omega_0 t + \varepsilon(t), \tag{1}$$

where γ is the damping factor and $\gamma > 0$, A and ω_0 are the amplitude and angular frequency of the periodic signal. x and t are moving trajectory of Brownian particles in $U(x)$ as time varies and time, respectively. $\varepsilon(t)$ is the Gaussian white noise. $U(x)$ is the harmonic-Gaussian double-well potential given by equation (2) and has richer dynamics than classical bistable potential. Therefore, it can be used to design the SR model enhanced by fractional-order derivative and time-delay feedback.

$$U(x) = \frac{k}{2}x^2 + \alpha\exp\left(-\beta x^2\right), \tag{2}$$

where k, α, and β are the adjusting parameters. The harmonic-Gaussian double-well potential has two stable states and one unstable state located at $x_\pm = \pm\sqrt{\ln(2\alpha\beta/k)/\beta}$ and $x_u = 0$, respectively. The height of potential barrier is $\Delta U = \alpha - k[1 + \ln(2\alpha\beta/k)]/(2\beta)$. To keep the bistability of harmonic-Gaussian double-well potential, $2\alpha\beta/k > 0$ and further $k < 2\alpha\beta$. The potential is plotted in Figure 1 under different tuning parameters. It can be found that when α and β are kept unchanged, tuning k can change the depth and width of double wells, as shown in Figure 1(a), where $k < 2\alpha\beta$. When k starts to become larger and $k > 2\alpha\beta$, the bistability of harmonic-Gaussian double-well potential loses becomes a monostable potential, as shown in Figure 1(b). Therefore, the following work would be performed under the condition of $k > 2\alpha\beta$.

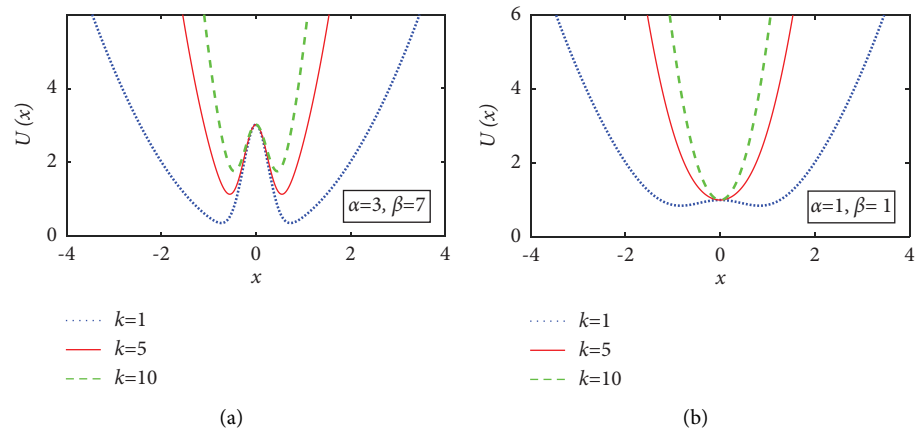

Figure 1: Harmonic-Gaussian double-well potentials under different adjusting parameters: (a) with $\alpha = 3$ and $\beta = 7$ and (b) with $\alpha = 1$ and $\beta = 1$.

Furthermore, the Grunwald–Letnikov fractional-order derivative [41, 42] is added into equation (1) as follows:

$$\frac{d^2x}{dt^2} + \gamma \frac{d^\vartheta x}{dt^\vartheta} = -\frac{\partial U(x)}{\partial x} + A\cos\omega_0 t + \varepsilon(t), \tag{3}$$

where ϑ is the fractional order and $\vartheta \in (0, 2]$ [43]. We rewrite equation (3) for numerical solution easily as follows:

$$\begin{cases} \dfrac{d^\vartheta x}{dt^\vartheta} = y, \\ \dfrac{d^2x}{dt^2} = \dfrac{d^\varphi y}{dt^\varphi}, \varphi = 2 - \vartheta, \\ \dfrac{d^\varphi y}{dt^\varphi} = -\gamma y - \dfrac{\partial U(x)}{\partial x} + A\cos\omega_0 t + \varepsilon(t). \end{cases} \tag{4}$$

According to the definition of the Grunwald–Letnikov fractional-order derivative, equation (4) can be transformed into the following discrete expression:

$$\begin{cases} x(l) = -\sum_{j=1}^{l-1} \omega_j^\vartheta x(l-j) + h^\vartheta y(l-1), \\ y(l) = -\sum_{j=1}^{l-1} \omega_j^\varphi y(l-j) + h^\varphi \left[-\gamma y(l-1) - kx(l-1) + 2\alpha\beta x(l-1)\exp\left(-\beta x^2(l-1)\right) + F(l-1)\right], \end{cases} \tag{5}$$

where $\omega_0^\vartheta = 1$, $\omega_l^\vartheta = [1 - (\vartheta + 1)/l]\omega_{l-1}^\vartheta$, and $l = 1, 2, \ldots, N$ in which N is the length or the number of sampling points of the signal $F(t) = A\cos\omega_0 t + \varepsilon(t)$. The variable h is the integral step. $x(l)$, $y(l)$, and $F(l)$ are the corresponding discrete expressions of $x(t)$, $y(t)$, and $F(t)$, respectively. It can be seen from equation (5) that adding the fractional-order derivative into the underdamped SR can make the current value of output $x(t)$ highly depend on historical values of the past. Due to the above reason, the fractional-order derivative can enhance the weak signal detection of SR. Moreover, such a property is consistent with a mechanical signal which has high dependence between each value.

Furthermore, we consider the memory of time delay to historical information and the precise control of feedback to the output of SR [44]. The time-delay feedback item is added into equation (4) to obtain the following equation:

$$\begin{cases} \dfrac{\mathrm{d}^{\vartheta}x(t)}{\mathrm{d}t^{\vartheta}} = y(t), \\ \dfrac{\mathrm{d}^{2}x(t)}{\mathrm{d}t^{2}} = \dfrac{\mathrm{d}^{\varphi}y(t)}{\mathrm{d}t^{\varphi}}, \varphi = 2-\vartheta, \\ \dfrac{\mathrm{d}^{\varphi}y(t)}{\mathrm{d}t^{\varphi}} = -\gamma y(t) - kx(t) + 2\alpha\beta x(t)\exp\left(-\beta x(t)^{2}\right) + \theta x(t-\tau) + F(t), \end{cases} \tag{6}$$

where $\theta > 0$ is the feedback strength and τ is the time delay. Equation (6) can be discretized to solve it numerically as follows:

$$\begin{cases} x(l) = -\sum_{j=1}^{l-1} \omega_j^{\vartheta} x(l-j) + h^{\vartheta} y(l-1), \\ y(l) = -\sum_{j=1}^{l-1} \omega_j^{\varphi} y(l-j), \\ + h^{\varphi}\left[-\gamma y(l-1) - kx(l-1) + 2\alpha\beta x(l-1)\exp\left(-\beta x^{2}(l-1)\right) + \theta x\left(l - \lfloor \tau f_s \rfloor\right) + F(l-1)\right], \end{cases} \tag{7}$$

where f_s is the sampling frequency and the notation $\lfloor \bullet \rfloor$ stands for round down. In equation (7), when $-\lfloor \tau/h \rfloor < 0$, $x(l - \lfloor \tau f_s \rfloor) = x(0) = 0$. According to the conclusions in [45, 46], the small delay is acceptable when $\tau < 1$.

Therefore, a SR model enhanced by fractional-order derivative and time-delay feedback is built in equation (6) and its numerical solution expression can be given by equation (7). In the model, there are eight tuning parameters to control the SR for enhancing weak signal detection, including fractional order $\vartheta \in (0, 2]$, damping factor $\gamma > 0$, harmonic-Gaussian double-well potential parameters including k, α, and β with the condition $k < 2\alpha\beta$, feedback strength θ, time delay $0 < \tau < 1$, and integral step $0 < h < 1$. Obviously, it is impossible for us to set up these tuning parameters artificially. For this purpose, we would use the optimization algorithms to tune these parameters automatically in this proposed method for enhancing weak fault signature of machinery.

3. Fractional-Order Derivative and Time-Delay Feedback Enabled Stochastic Resonance for Bearing Fault Diagnosis

In this section, we would propose an adaptive SR method based on the model built in Section 2 to enhance weak fault signature for identification. Moreover, an experiment on bearing faults was performed to verify the feasibility and effectiveness of the proposed method.

3.1. The Proposed Method. The proposed fractional-order derivative and time-delay feedback enabled stochastic resonance method for bearing fault diagnosis is shown in Figure 2 and the detailed processes are given as follows:

(1) Parameter initialization: The proposed method is based on the SR model built in equation (6) and, therefore, it has eight tuning parameters including fractional order ϑ, damping factor γ, potential parameters k, α and β, feedback strength θ, time delay τ, and integral step h. According to their definitions and physical meanings, they are initialized as $\vartheta \in (0, 2]$, $\gamma \in (0, +\infty]$, $k \in (0, +\infty]$, $\alpha \in (0, +\infty]$, $\beta \in (0, +\infty]$, $\theta \in (0, +\infty]$, $\tau \in (0, 1)$, and $h \in (0, 1)$, respectively.

(2) Output solution: The vibration signal $F(t)$ of bearings with the sampling frequency f_s and the data length N is fed into equation (6). Then, the output $x(l)$ can be calculated by using equation (7) where $l = 1, 2, \cdots, N$. In the solving process, the initialization values of these tuning parameters including ϑ, γ, k, α, β, θ, τ, and h would be substituted into equation (7) for solving $x(l)$.

(3) Parameter optimization: According to equation (8), we can calculate the local signal-to-noise ratio (LSNR) of the output $x(l)$ as an objective function of the genetic algorithms. For fault diagnosis of machines, the intensity of fault signature in the local frequency band would be cared instead of the whole

frequency band. Therefore, LSNR indicator has more meaning to evaluate weak fault signature enhanced by SR. Furthermore, the solving issue can be transformed into the following optimal issue in equation (9).

$$\mathrm{LSNR} = 20\log\frac{A\left(\lfloor f_c \times N/f_s \rfloor + 1\right)}{\sum_{i=\lfloor f_c \times N/f_s \rfloor + 1 - M}^{i=\lfloor f_c \times N/f_s \rfloor + 1 + M} A(i)}, \tag{8}$$

where $A(i)$ denotes the amplitude at i-th spectral line of the frequency spectrum of the output signal $x(l)$ and M is the tuning range for selecting a local frequency band, and here $M = 50$. f_c denotes the theoretical value of the fault characteristic frequency of bearings, which can be calculated by virtue of structural parameters and operating speed of bearings.

$$\max_{\vartheta,\gamma,k,\alpha,\beta,\theta,\tau,h} \mathrm{LSNR}\ \text{s.t.} \begin{cases} \vartheta \in (0, 2], \\ \gamma \in (0, +\infty], \\ k \in (0, +\infty], \\ \alpha \in (0, +\infty], \\ \beta \in (0, +\infty], \\ \theta \in (0, +\infty], \\ \tau \in (0, 1), \\ h \in (0, 1), \end{cases} \tag{9}$$

(4) Optimal output calculation and fault identification. The optimal parameter set for maximizing the LSNR is substituted into equation (7) for solving $x_{\mathrm{opt}}(l)$. Then, common spectral analysis such as frequency spectrum and envelope spectrum is performed on the $x_{\mathrm{opt}}(l)$ to recognize the weak fault signature of roller bearings, which especially pays close attention to the spectral peaks at the fault characteristic frequencies of the bearings.

3.2. Experimental Verification. In this subsection, the proposed fractional-order derivative and time-delay feedback enabled stochastic resonance method is applied to bearing fault diagnosis for verifying its feasibility and effectiveness. Due to contact fatigue, uneven lubrication, misalignment, and so on, it is inevitable for roller bearings to occur wears and other types of defects [47–49]. In early stage of defects, the changes of vibration and oil temperature of bearings are too weak to be visible to the naked eye [50]. In serious stage of defects, the changes of vibration and oil temperature of bearings are very clear to be observed by ears and fingers [51]. Therefore, it is a challenge for us to detect the early defects of bearings by using advanced methods and technologies. For this purpose, we would apply the proposed method to early fault diagnosis of bearings.

Four Rexnord ZA-2115 double row bearing run-to-failure experiments under the rotating speed 2000 rpm and radial load 6000 lbs were performed to acquire the bearing failure data by using PCB 353B33 accelerometers and a data acquisition card. The bearing experimental rig is shown in Figure 3(a) and the corresponding sensor placement is illustrated in Figure 3(b). This experimental rig is composed of four tested bearings, an AC motor, and rub belts. In the bearing run-to-failure experiment, the sampling frequency is 20 kHz and the sampling time is 1.024 seconds. The experimental parameters of tested bearing are shown in Table 1. In the process of experiment, an inner race defect occurs on the tested bearing 3, as shown in Figure 3(c). According to the equation that $f_{\mathrm{inner}} = r_{\mathrm{speed}}/60 * 1/2 * n(1 + d/D\cos\psi)$, where f_{inner} is inner race fault characteristic frequency, r_{speed} is the rotating speed, n is the number of rollers, d is the roller diameter, D is the pitch diameter, and ψ is the contact angle, and the theoretical inner race fault characteristic frequency $f_{\mathrm{inner}} = 296.93$ Hz.

The time-domain signal collected from a bearing usually changes when a damage occurs in a bearing. Both its amplitude and distribution may be different from those of the time-domain signal of a normal bearing. Root mean square (RMS) reflects the vibration amplitude and energy in time domain [53]. Figure 4(a) depicts the RMS of the tested bearing 3. It can be found from Figure 4(a) that the RMS starts to be stable and then becomes larger slowly and finally degenerates rapidly. To the end, a serious defect occurred on the tested bearing 3. Therefore, we choose the vibration signal at the early stage of defects to perform the spectral analysis, as shown in Figure 4(b). From the raw signal, we can see weak impacts but they are submerged by strong noise. In Figure 4(c), there are clear spectrum peaks at 232.5 Hz, 493.8 Hz, etc., but we cannot see the spectral peaks at the inner race fault characteristic frequency and its harmonics. Meanwhile, we also cannot see the corresponding spectral peaks from the zoomed envelope spectrum in Figure 4(d).

The raw signal in Figure 4(b) is fed into the proposed method and the underdamped SR without both fractional derivative and time-delay feedback to enhance weak fault signature, respectively. The enhanced results are plotted in Figure 5. It can be found that there are clear repetitive impacts in the time-domain signal as shown in Figure 5(a) and we can see the eye-catching spectral peaks at the inner race fault characteristic frequency and its harmonics from the corresponding frequency spectrum in Figure 5(b) and even side frequency bands with the interval rotating frequency. The above information tells us the fact that an inner race wear has happened in the tested bearing 3. The diagnosis results are consistent with the experimental results. Meanwhile, Figures 5(c) and 5(d) show the enhanced signal and its zoomed frequency spectrum by using the underdamped SR without both fractional derivative and time-delay feedback, where the objective function is usually SNR instead of LSNR. It can be noticed that there exists a eye-catching spectral peak at the inner race fault characteristic frequency, but we cannot see other any diagnostic information, that is, because the SNR indicator would be calculated by the ratio between the energy at the inner race fault characteristic frequency and the energy at the whole frequency band in addition to fault signature, resulting in energy concentration and ignoring other diagnostic information. Moreover, the spectral peak at the inner race fault

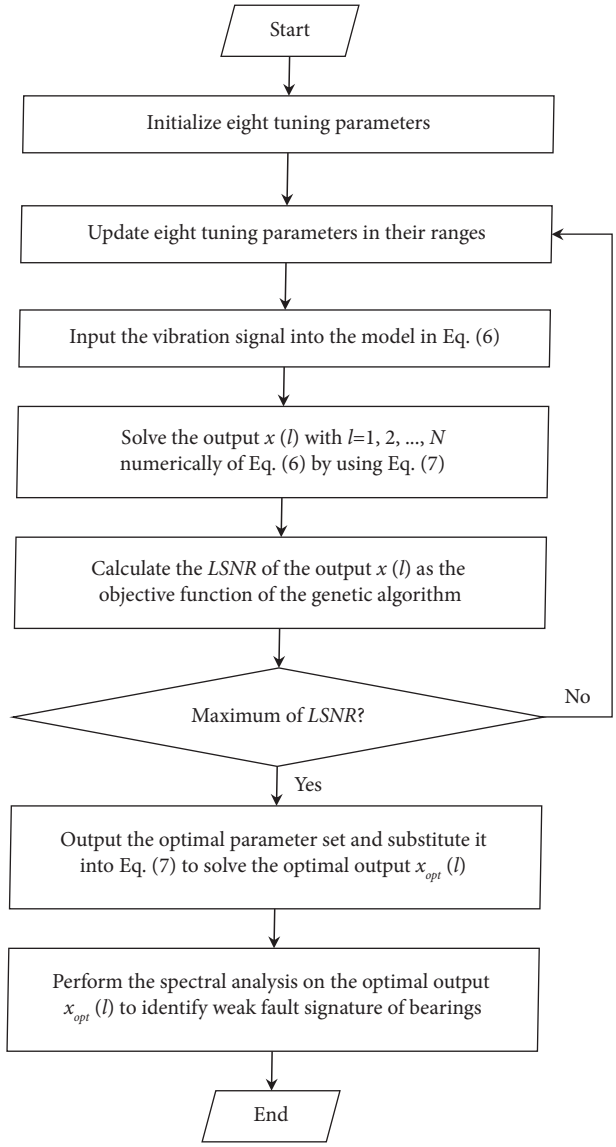

Figure 2: The flowchart of the proposed method.

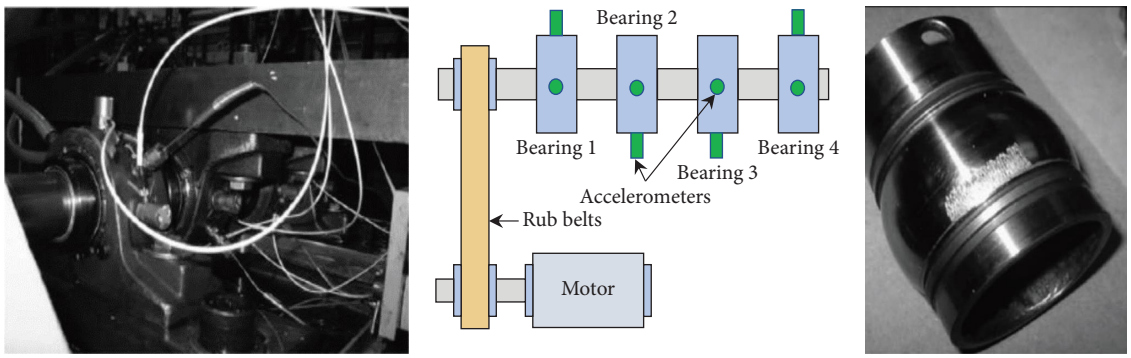

Figure 3: Bearing test rigs and sensor placement illustration: (a) bearing test rigs, (b) sensor placement illustration, and (c) the tested bearing with an inner race wear [52].

Table 1: Experimental parameters of tested bearings.

Parameters	Values
Rotating speed	2000 rpm
Pitch diameter	2.815 in
Number of balls	16
Sampling frequency	20 kHz
Roller diameter	0.331 in
Contact angle	15.17°

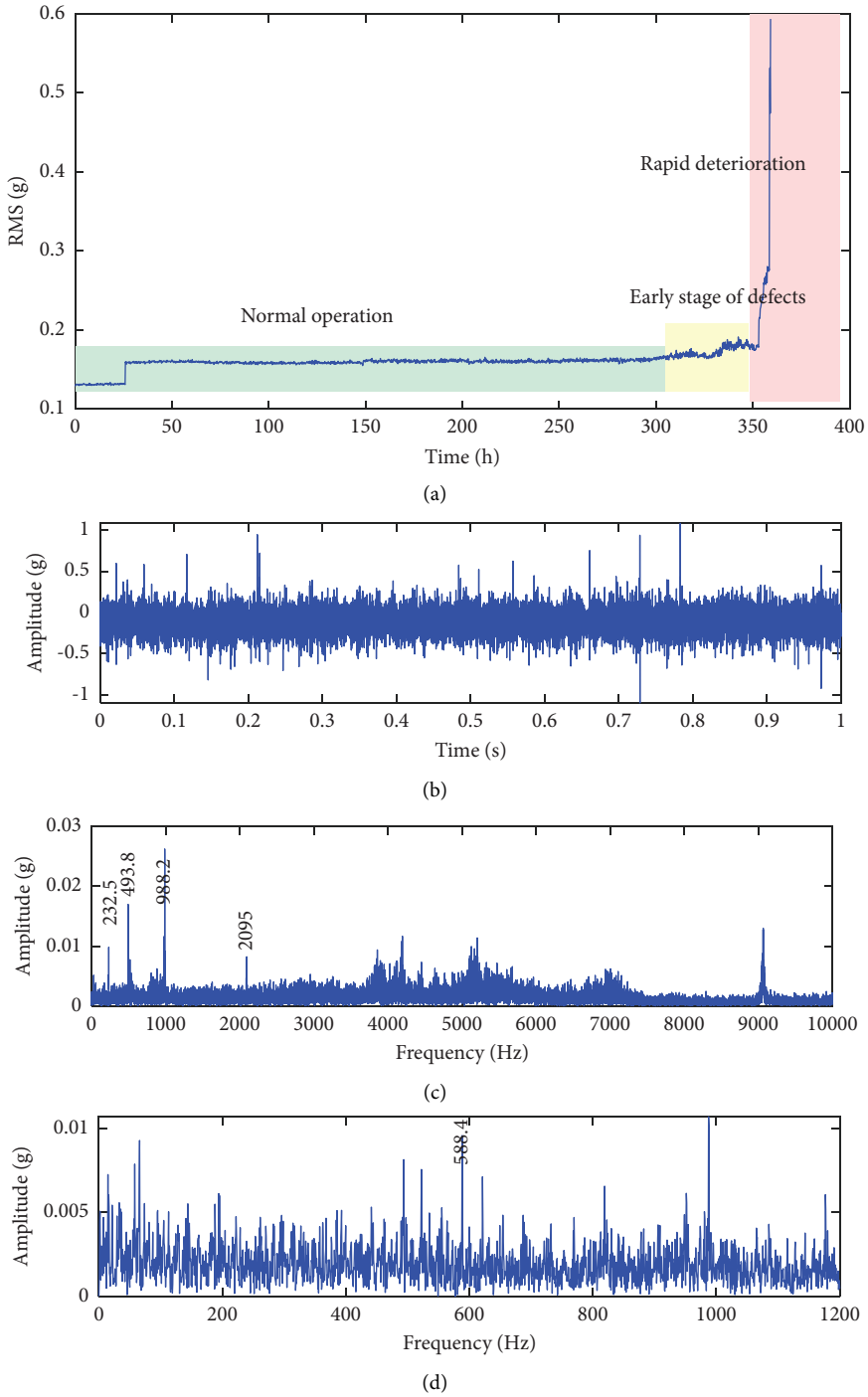

Figure 4: The RMS and raw signal of the tested bearing 3: (a) the RMS, (b) raw signal, (c) frequency spectrum, and (d) zoomed envelope spectrum.

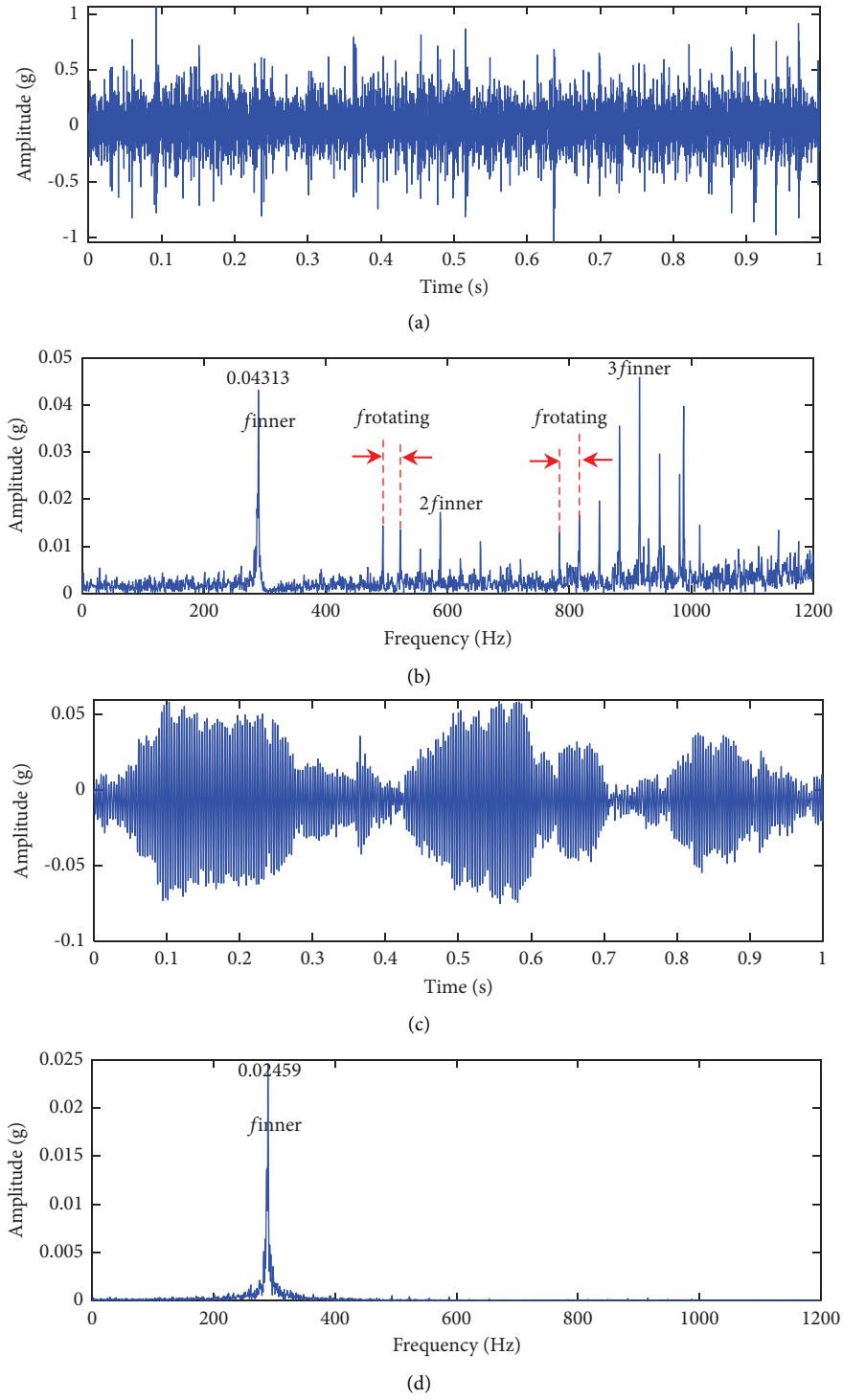

Figure 5: The enhanced result and its spectrum using the proposed method and underdamped SR without both fractional derivative and time-delay feedback: (a) time-domain signal and (b) its zoomed frequency spectrum using the proposed method and (c) time-domain signal and (d) its zoomed frequency spectrum using underdamped SR without both fractional derivative and time-delay feedback.

characteristic frequency using the proposed method is higher than that one using underdamped SR without both fractional derivative and time-delay feedback. The above comparison demonstrates that the proposed method has richer diagnostic information and higher spectral peak at the inner race fault characteristic frequency than underdamped SR without both fractional derivative and time-delay feedback.

For comparison, the advanced infogram method [54–56] is applied to process the raw vibration signal in Figure 4(b), and the infogram for selecting the most informative frequency band is shown in Figure 6. It can be seen that the SE

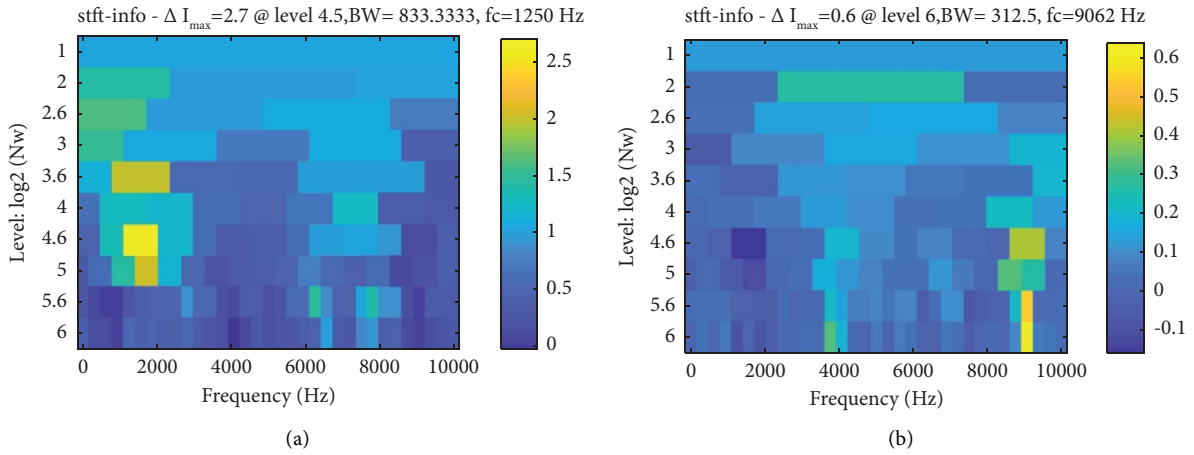

Figure 6: The infogram: (a) SE infogram and (b) SES infogram.

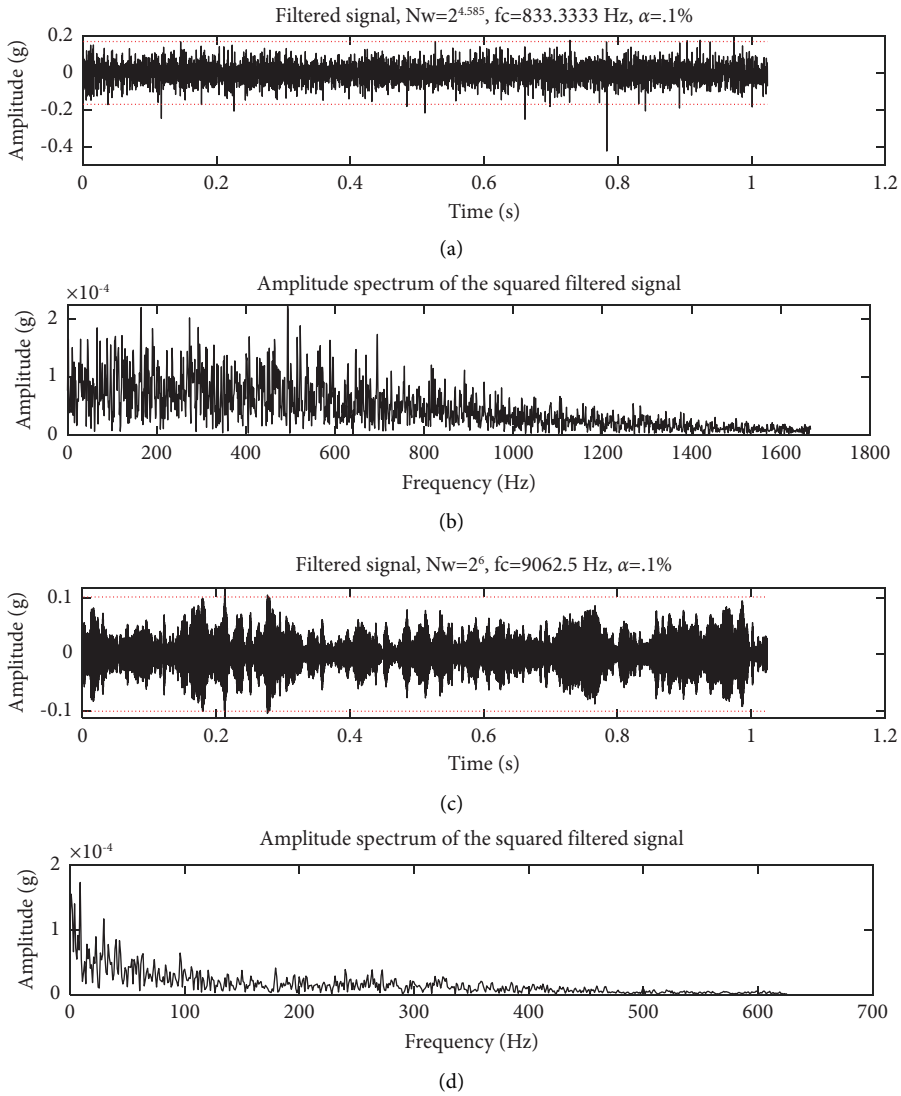

Figure 7: The detected results using infogram: (a) the filtered signal and (b) its amplitude spectrum using SE infogram and (c) the filtered signal and (d) its amplitude spectrum using SES infogram.

infogram in Figure 6(a) and SES infogram in Figure 6(b) select different filtered frequency band and its parameters. Therefore, we apply two filtered frequency bands to filter the raw signal and the results are depicted in Figure 7. It can be seen that the SE infogram filters out the cyclostationary information as shown in Figure 7(a), but we cannot see the peaks at the inner race fault characteristic frequency and its harmonics from Figure 7(b). On the contrary, the SES infogram filters out the impulsivity information as shown in Figure 7(c), but we cannot also see the peaks at the inner race fault characteristic frequency and its harmonics from Figure 7(d). The comparison with other non-SR methods demonstrates the feasibility and superiority of the proposed method further.

4. Conclusions

Stochastic resonance (SR) has become a hot signal processing method and has been widely used in mechanical fault diagnosis, such as fractional-order SR and time-delayed feedback SR. Here, fractional-order SR can utilize the historical information to enhance weak fault signature, and time delay and feedback can improve the memory of SR and tune it precisely. Therefore, we attempt to fuse fractional-order derivative and time-delayed feedback to develop the better SR method. Inspired by the idea, fractional-order derivative and time-delay feedback enabled SR method for bearing fault diagnosis is proposed in this paper. The comparison with the advanced infogram and the SR without fractional-order derivative and time-delay feedback is made. The results indicate that the proposed method has a little superiority in enhancing weak fault signature and richer diagnostic information in the enhanced results than the SR without fractional-order derivative and time-delay feedback. In future work, we would pay more attention to design SR-based filters to take the place of filters in infogram for exploring the SR-based infogram.

Data Availability

The data used in this study are available on request from the corresponding author.

Conflicts of Interest

The authors declare that they have no conflicts of interest.

Authors' Contributions

Yidan Mei conducted the experimental work, performed data analysis, provided theoretical explanations, and drafted the manuscript. Lutie Chen and Wentao Xu provided valuable feedback and constructive suggestions. Chao Liu and Zijian Qiao conducted a thorough review and made substantial revisions to the technical paper. Zhihui Lai contributed to the linguistic accuracy and fluency of the academic manuscript.

Acknowledgments

This research was supported by the Zhejiang Provincial Natural Science Foundation of China (LQ22E050003), Ningbo Natural Science Foundation (2022J132), National Natural Science Foundation of China (52205569), Chuying Planning Project of Zhejiang Provincial Administration for Market Regulation (CY2023328), Ningbo Science and Technology Major Project (2023Z133), and Laboratory of Yangjiang Offshore Wind Power (YJOFWD-OF-2022A08), and also sponsored by K.C. Wong Magna Fund in Ningbo University.

References

[1] L. Gammaitoni, P. Hänggi, P. Jung, and F. Marchesoni, "Stochastic resonance," *Reviews of Modern Physics*, vol. 70, no. 1, pp. 223–287, 1998.

[2] K. Wiesenfeld and F. Moss, "Stochastic resonance and the benefits of noise: from ice ages to crayfish and SQUIDs," *Nature*, vol. 373, no. 6509, pp. 33–36, 1995.

[3] Y. Ding, Y. Kang, and Y. Zhai, "Rolling bearing fault diagnosis based on exact moment dynamics for underdamped periodic potential systems," *IEEE Transactions on Instrumentation and Measurement*, vol. 72, pp. 1–12, 2023.

[4] N. Murray and M. Holman, "The role of chaotic resonances in the solar system," *Nature*, vol. 410, no. 6830, pp. 773–779, 2001.

[5] Y. He, Y. Fu, Z. Qiao, and Y. Kang, "Chaotic resonance in a fractional-order oscillator system with application to mechanical fault diagnosis," *Chaos, Solitons & Fractals*, vol. 142, Article ID 110536, 2021.

[6] I. T. Tokuda, C. E. Han, K. Aihara, M. Kawato, and N. Schweighofer, "The role of chaotic resonance in cerebellar learning," *Neural Networks*, vol. 23, no. 7, pp. 836–842, 2010.

[7] S. Ghosh and D. S. Ray, "Nonlinear vibrational resonance," *Physical Review*, vol. 88, no. 4, Article ID 042904, 2013.

[8] V. S. Rallabandi and P. K. Roy, "Magnetic resonance image enhancement using stochastic resonance in Fourier domain," *Magnetic Resonance Imaging*, vol. 28, no. 9, pp. 1361–1373, 2010.

[9] N. G. Stocks, "Information transmission in parallel threshold arrays: suprathreshold stochastic resonance," *Physical Review*, vol. 63, no. 4, Article ID 041114, 2001.

[10] S. Lu, Q. He, and J. Wang, "A review of stochastic resonance in rotating machine fault detection," *Mechanical Systems and Signal Processing*, vol. 116, pp. 230–260, 2019.

[11] Y. Lei, Z. Qiao, X. Xu, J. Lin, and S. Niu, "An underdamped stochastic resonance method with stable-state matching for incipient fault diagnosis of rolling element bearings," *Mechanical Systems and Signal Processing*, vol. 94, pp. 148–164, 2017.

[12] A. Elhattab, N. Uddin, and E. Obrien, "Drive-by bridge frequency identification under operational roadway speeds employing frequency independent underdamped pinning stochastic resonance (FI-UPSR)," *Sensors*, vol. 18, no. 12, p. 4207, 2018.

[13] Y. G. Leng, Y. S. Leng, T. Y. Wang, and Y. Guo, "Numerical analysis and engineering application of large parameter stochastic resonance," *Journal of Sound and Vibration*, vol. 292, no. 3-5, pp. 788–801, 2006.

[14] Z. Qiao, Y. Lei, and N. Li, "Applications of stochastic resonance to machinery fault detection: a review and tutorial,"

Mechanical Systems and Signal Processing, vol. 122, pp. 502–536, 2019.

[15] X. Huang, "Stochastic resonance in a piecewise bistable energy harvesting model driven by harmonic excitation and additive Gaussian white noise," *Applied Mathematical Modelling*, vol. 90, pp. 505–526, 2021.

[16] C. B. Güngör, P. P. Mercier, and H. Töreyin, "A stochastic resonance electrocardiogram enhancement algorithm for robust QRS detection," *IEEE Journal of Biomedical and Health Informatics*, vol. 26, no. 8, pp. 3743–3754, 2022.

[17] W. Zhang, P. Shi, M. Li, and D. Han, "A novel stochastic resonance model based on bistable stochastic pooling network and its application," *Chaos, Solitons & Fractals*, vol. 145, Article ID 110800, 2021.

[18] S. Bai, F. Duan, F. Chapeau-Blondeau, and D. Abbott, "Generalization of stochastic-resonance-based threshold networks with Tikhonov regularization," *Physical Review*, vol. 106, no. 1, Article ID L012101, 2022.

[19] Y. Zheng, M. Huang, Y. Lu, and W. Li, "Fractional stochastic resonance multi-parameter adaptive optimization algorithm based on genetic algorithm," *Neural Computing & Applications*, vol. 32, no. 22, pp. 16807–16818, 2020.

[20] J. H. Yang, M. A. F. Sanjuán, H. G. Liu, G. Litak, and X. Li, "Stochastic P-bifurcation and stochastic resonance in a noisy bistable fractional-order system," *Communications in Nonlinear Science and Numerical Simulation*, vol. 41, pp. 104–117, 2016.

[21] X. Zeng, X. Lu, Z. Liu, and Y. Jin, "An adaptive fractional stochastic resonance method based on weighted correctional signal-to-noise ratio and its application in fault feature enhancement of wind turbine," *ISA Transactions*, vol. 120, pp. 18–32, 2022.

[22] Z. Qiao, A. Elhattab, X. Shu, and C. He, "A second-order stochastic resonance method enhanced by fractional-order derivative for mechanical fault detection," *Nonlinear Dynamics*, vol. 106, no. 1, pp. 707–723, 2021.

[23] F. Guo, C. Y. Zhu, X. F. Cheng, and H. Li, "Stochastic resonance in a fractional harmonic oscillator subject to random mass and signal-modulated noise," *Physica A: Statistical Mechanics and Its Applications*, vol. 459, pp. 86–91, 2016.

[24] T. Yu, L. Zhang, Y. Ji, and L. Lai, "Stochastic resonance of two coupled fractional harmonic oscillators with fluctuating mass," *Communications in Nonlinear Science and Numerical Simulation*, vol. 72, pp. 26–38, 2019.

[25] S. Zhong, W. Lv, H. Ma, and L. Zhang, "Collective stochastic resonance behavior in the globally coupled fractional oscillator," *Nonlinear Dynamics*, vol. 94, no. 2, pp. 905–923, 2018.

[26] D. Wu and S. Zhu, "Stochastic resonance in a bistable system with time-delayed feedback and non-Gaussian noise," *Physics Letters A*, vol. 363, no. 3, pp. 202–212, 2007.

[27] S. Lu, Q. He, H. Zhang, and F. Kong, "Enhanced rotating machine fault diagnosis based on time-delayed feedback stochastic resonance," *Journal of Vibration and Acoustics*, vol. 137, no. 5, 2015.

[28] P. Shi, D. Yuan, D. Han, Y. Zhang, and R. Fu, "Stochastic resonance in a time-delayed feedback tristable system and its application in fault diagnosis," *Journal of Sound and Vibration*, vol. 424, pp. 1–14, 2018.

[29] P. Shi, W. Zhang, D. Han, and M. Li, "Stochastic resonance in a high-order time-delayed feedback tristable dynamic system and its application," *Chaos, Solitons & Fractals*, vol. 128, pp. 155–166, 2019.

[30] Y. J. Wadop Ngouongo, M. Djolieu Funaye, G. Djuidjé Kenmoé, and T. C. Kofané, "Stochastic resonance in deformable potential with time-delayed feedback," *Philosophical Transactions of the Royal Society A: Mathematical, Physical & Engineering Sciences*, vol. 379, no. 2192, Article ID 20200234, 2021.

[31] Q. B. Wang, H. Wu, and Y. J. Yang, "The effect of fractional damping and time-delayed feedback on the stochastic resonance of asymmetric SD oscillator," *Nonlinear Dynamics*, vol. 107, no. 3, pp. 2099–2114, 2022.

[32] J. Li, M. Li, and J. Zhang, "Rolling bearing fault diagnosis based on time-delayed feedback monostable stochastic resonance and adaptive minimum entropy deconvolution," *Journal of Sound and Vibration*, vol. 401, pp. 139–151, 2017.

[33] N. Wang, A. Song, and B. Yang, "The effect of time-delayed feedback on logical stochastic resonance," *The European Physical Journal B*, vol. 90, no. 6, pp. 117–125, 2017.

[34] T. Yang and Q. Cao, "Delay-controlled primary and stochastic resonances of the SD oscillator with stiffness nonlinearities," *Mechanical Systems and Signal Processing*, vol. 103, pp. 216–235, 2018.

[35] J. Liu, B. Hu, F. Yang, C. Zang, and X. Ding, "Stochastic resonance in a delay-controlled dissipative bistable potential for weak signal enhancement," *Communications in Nonlinear Science and Numerical Simulation*, vol. 85, Article ID 105245, 2020.

[36] Z. Qiao, S. Chen, Z. Lai, S. Zhou, and M. A. F. Sanjuán, "Harmonic-Gaussian double-well potential stochastic resonance with its application to enhance weak fault characteristics of machinery," *Nonlinear Dynamics*, vol. 111, no. 8, pp. 7293–7307, 2023.

[37] Z. Liao, Z. Wang, H. Yamahara, and H. Tabata, "Low-power-consumption physical reservoir computing model based on overdamped bistable stochastic resonance system," *Neurocomputing*, vol. 468, pp. 137–147, 2022.

[38] H. L. He, T. Y. Wang, Y. G. Leng, Y. Zhang, and Q. Li, "Study on non-linear filter characteristic and engineering application of cascaded bistable stochastic resonance system," *Mechanical Systems and Signal Processing*, vol. 21, no. 7, pp. 2740–2749, 2007.

[39] S. Lu, Q. He, and F. Kong, "Effects of underdamped step-varying second-order stochastic resonance for weak signal detection," *Digital Signal Processing*, vol. 36, pp. 93–103, 2015.

[40] Z. Qiao, J. Liu, X. Ma, and J. Liu, "Double stochastic resonance induced by varying potential-well depth and width," *Journal of the Franklin Institute*, vol. 358, no. 3, pp. 2194–2211, 2021.

[41] J. A. Tenreiro Machado, "A probabilistic interpretation of the fractional-order differentiation," *Fractional Calculus and Applied Analysis*, vol. 6, pp. 73–79, 2003.

[42] D. W. Brzeziński and P. Ostalczyk, "About accuracy increase of fractional order derivative and integral computations by applying the Grünwald-Letnikov formula," *Communications in Nonlinear Science and Numerical Simulation*, vol. 40, pp. 151–162, 2016.

[43] C. Wu, S. Lv, J. Long, J. Yang, and M. A. F. Sanjuán, "Self-similarity and adaptive aperiodic stochastic resonance in a fractional-order system," *Nonlinear Dynamics*, vol. 91, no. 3, pp. 1697–1711, 2018.

[44] X. Yun, X. Mei, and G. Jiang, "Time-delayed feedback stochastic resonance enhanced minimum entropy deconvolution for weak fault detection of rolling element bearings," *Chinese Journal of Physics*, vol. 76, pp. 1–13, 2022.

[45] R. H. Shao and Y. Chen, "Stochastic resonance in time-delayed bistable systems driven by weak periodic signal," *Physica A: Statistical Mechanics and Its Applications*, vol. 388, no. 6, pp. 977–983, 2009.

[46] S. Guillouzic, I. L'Heureux, and A. Longtin, "Small delay approximation of stochastic delay differential equations," *Physical Review*, vol. 59, no. 4, pp. 3970–3982, 1999.

[47] Z. Qiao and X. Shu, "Coupled neurons with multi-objective optimization benefit incipient fault identification of machinery," *Chaos, Solitons & Fractals*, vol. 145, Article ID 110813, 2021.

[48] Z. Qiao and Z. Pan, "SVD principle analysis and fault diagnosis for bearings based on the correlation coefficient," *Measurement Science and Technology*, vol. 26, no. 8, Article ID 085014, 2015.

[49] R. B. Randall and J. Antoni, "Why EMD and similar decompositions are of little benefit for bearing diagnostics," *Mechanical Systems and Signal Processing*, vol. 192, Article ID 110207, 2023.

[50] Y. Xu, D. Zhen, J. X. Gu et al., "Autocorrelated envelopes for early fault detection of rolling bearings," *Mechanical Systems and Signal Processing*, vol. 146, Article ID 106990, 2021.

[51] M. Xu, C. Zheng, K. Sun, L. Xu, Z. Qiao, and Z. Lai, "Stochastic resonance with parameter estimation for enhancing unknown compound fault detection of bearings," *Sensors*, vol. 23, no. 8, p. 3860, 2023.

[52] H. Qiu, J. Lee, J. Lin, and G. Yu, "Wavelet filter-based weak signature detection method and its application on rolling element bearing prognostics," *Journal of Sound and Vibration*, vol. 289, no. 4-5, pp. 1066–1090, 2006.

[53] Y. Lei, M. J. Zuo, Z. He, and Y. Zi, "A multidimensional hybrid intelligent method for gear fault diagnosis," *Expert Systems with Applications*, vol. 37, no. 2, pp. 1419–1430, 2010.

[54] J. Antoni, "The infogram: entropic evidence of the signature of repetitive transients," *Mechanical Systems and Signal Processing*, vol. 74, pp. 73–94, 2016.

[55] C. Li, D. Cabrera, J. V. De Oliveira, R. Sanchez, M. Cerrada, and G. Zurita, "Extracting repetitive transients for rotating machinery diagnosis using multiscale clustered grey infogram," *Mechanical Systems and Signal Processing*, vol. 76, pp. 157–173, 2016.

[56] X. Xu, Z. Qiao, and Y. Lei, "Repetitive transient extraction for machinery fault diagnosis using multiscale fractional order entropy infogram," *Mechanical Systems and Signal Processing*, vol. 103, pp. 312–326, 2018.